Available online at www.sciencedirect.com
SCIENCE DIRECT
International Journal of Heat and Mass Transfer 49 (2006) 3645–3654
International Journal of HEAT and MASS TRANSFER
www.elsevier.com/locate/ijhmt

Thermal protection with liquid film in turbulent mixed convection channel flows

Jer-Huan Jang [a], Wei-Mon Yan [b,*]

[a] Department of Mechanical Engineering, Northern Taiwan Institute of Science and Technology, Pei-To, Taipei 112, Taiwan, ROC
[b] Department of Mechatronic Engineering, Graduate Institute of Mechatronic Engineering, Huafan University, Shih-Ting, Taipei 223, Taiwan, ROC

Received 8 September 2005; received in revised form 19 February 2006
Available online 18 April 2006

Abstract

In this numerical study, a channel flow of turbulent mixed convection of heat and mass transfer with film evaporation has been conducted. The turbulent hot air flows downward of the vertical channel and is cooled by the laminar liquid film on both sides of the channel with thermally insulated walls. The effect of gas–liquid phase coupling, variable thermophysical properties and film vaporization are considered in the analysis. In the air stream, the k–ε turbulent model has been utilized to formulate the turbulent flow. Parameters used in this study are the mass flow rate of the liquid film B, Reynolds number Re, and the free stream temperature of the hot air T_o. Results show that the heat flux was dramatically increases due to the evaporation of liquid water film. The heat transfer increases as the mass flow rate of the liquid film decreases, while the Reynolds number and inlet temperature increase, and the influences of the Re and T_o are more significant than that of the liquid flow rate. It is also found that liquid film helps lowering the heat and mass transfer rate from the hot gas in the turbulent channel, especially at the downstream.

1. Introduction

Increasing the maximum temperature of a cycle can improve both the efficiency and the specific power of continuous fluxes motors such as gas turbines, and rocket nozzle. It also has to raise the thermal resistance at high temperature of the material used exposed to the hot gases. However, the thermal resistance of the material can reach to its limits, so it is required to cool adequately the exposed surfaces of thermal resistance material. Wall cooling is an essential element in the protection of surfaces exposed to high temperatures. Different techniques can be used for protecting surfaces. Porous media, moist fire-protection materials, discrete injection and falling film are some examples.

Falling film technology has been utilized in many engineering application, both experimental works and theoretical analyses have been conducted over the last few decades [1]. Several parameters can influence the cooling system: the cooling fluid can be chemically different from the main flow; the film flow rate can vary and changes the behavior of the boundary layer. Baumann and Thiele [2] considered the evaporation of a binary liquid film flowing inside a cylindrical duct. For liquid benzene–methanol mixtures into a hot air stream, they show that small portions of a second component in the liquid film can create significant changes in the temperature levels as well as in the heat and mass transfer. Ali Cherif and Daïf [3] considered the evaporation of a thin binary liquid film by mixed convection in a vertical channel. They showed the importance of the film thickness and composition in the mass and heat transfers.

Due to its importance, numerous works investigated numerically and experimentally on the liquid film evaporation [4–11]. Several of the earlier studies focused on heat and mass transfer in the gas flow, in which the very thin liquid film was assumed to be replaced by appropriate boundary conditions. Therefore, the results produced are valid only for a system with extremely thin films [12,13].

* Corresponding author. Tel.: +886 2 2663 2102; fax: +886 2 2663 1119.
E-mail address: wmyan@huafan.hfu.edu.tw (W.-M. Yan).

0017-9310/$ - see front matter © 2006 Elsevier Ltd. All rights reserved.
doi:10.1016/j.ijheatmasstransfer.2006.02.037

Nomenclature

b	half-channel width (m)
B	mass flow rate of the liquid film (kg m^{-1} s^{-1})
C_1	constant in turbulent k–ε model
C_2	constant in turbulent k–ε model
C_μ	constant in turbulent k–ε model
C_p	specific heat (J kg^{-1} K^{-1})
D	mass diffusivity (m^2 s^{-1})
f_2	function in turbulent k–ε model
f_μ	function in turbulent k–ε model
g	gravitational acceleration (m s^{-2})
h	heat transfer coefficient
h_{fg}	latent heat of vaporization (J kg^{-1})
h_M	mass transfer coefficient
k	turbulent kinetic energy (m^2 s^{-2})
M_a	molar mass of air (kg mol^{-1})
M_v	molar mass of water vapor (kg mol^{-1})
$\dot{m}''_I$	evaporating mass flux (kg s^{-1} m^{-2})
Nu_l	local Nusselt number for latent heat transfer, Eq. (18)
Nu_s	local Nusselt number for sensible heat transfer, Eq. (17)
Nu_x	overall Nusselt number, Eq. (15)
p	mixture pressure (kPa)
p_I	partial pressure of water vapor at the gas–liquid interface (kPa)
p_m	motion pressure, p–p_o
q''_I	total interfacial energy flux, Eq. (14) (W m^{-2})
q''_{ll}	latent heat flux, $\dot{m}''_I \cdot h_{fg}$ (W m^{-2})
q''_{sI}	sensible heat flux (W m^{-2})
Re	gas stream Reynolds number, $\frac{\bar{u}_f \cdot 4b}{\nu_o}$
R_t	turbulent Reynolds number, $\frac{k^2}{\nu\varepsilon}$
Sh	local Sherwood number
T	temperature (K)
T_{li}	inlet temperature of liquid film (K)
T_o	inlet temperature of hot air stream (K)
u	axial velocity (m s^{-1})
u^*	shear stress velocity, $(\tau_w/\rho)^{1/2}$
u_f	fully developed velocity at inlet (m s^{-1})
$\bar{u}_f$	average inlet velocity (m s^{-1})
v	transverse velocity (m s^{-1})
w	mass fraction of water vapor
x	coordinate in the flow direction (m)
X	dimensionless axial location, x/b
y	coordinate in the transverse direction (m)
Y	dimensionless wall coordinate, $(b - y - \delta)u^*/\nu$

Greek symbols

δ	local liquid film thickness (m)
ε	the rate of dissipation of turbulent kinetic energy (m^2 s^{-3})
λ	molecular thermal conductivity (W m^{-1} K^{-1})
μ	molecular dynamic viscosity (kg m^{-1} s^{-1})
ρ	density (kg m^{-3})
σ_k	turbulent Prandtl number for k
σ_ε	turbulent Prandtl number for ε
τ	shear stress (kPa)

Subscripts

b	bulk quantity
g	mixture (air + water vapor)
I	condition at gas–liquid interfaces
l	liquid film
o	condition at inlet
t	turbulent
w	condition at wall

The transport process in both gas flow and liquid film has been analyzed by Shembharkar and Pai [14], Baumann and Thiele [15], Yan [16], and Tsay and Lin [17]. Although they considered turbulent gas flow, liquid film was still assumed as laminar. The major difference among them was the definition of liquid film temperature profile. The first two assumed the temperature profile across the film was linear, and the later two considered the profile as fully developed laminar.

The aiding-buoyancy force on turbulent force convection heat transfer in a vertical pipe was examined by Carr et al. [18] and Connor and Carr [19]. Their results showed that a limiting profile shape was approached at high Grashof numbers with the maximum velocity shifting towards the heated wall. The effects of opposing-buoyancy force on the characteristic of flow and heat transfer in turbulent pipe flow were investigated by Axcell and Hall [20] and Easby [21]. They found remarkable enhancements in heat transfer rate but a decrease in the friction compared with the corresponding results of turbulent forced convection. As far as mixed convection heat and mass transfer is concerned, Yan and his colleagues [22–25] explored the evaporative cooling of liquid falling film in laminar natural or mixed convection channel flows as well as Feddaoui et al. [26]. However, heat and mass transfer over a vaporizing liquid film is always encountered in a turbulent convection flow in practical applications. Later, researches of turbulent mixed convection of heat and mass transfer with film evaporation have been conducted by several investigators [27–29]. In these studies, the liquid film was laminar and served as an enhancement of cooling with heating from outside of computational domain.

The objective of the present study is to analyze the turbulent mixed convection heat and mass transfer processes in moving laminar liquid film. Two-dimensional incompressible boundary layer model is employed for liquid film and gas flows. The effects of inlet conditions on the performance of falling film evaporation are examined.

The parametric study is focused on the effects of gas velocity and temperature as well as the liquid mass flow rate.

2. Analysis

The present study deals with a numerical analysis of water evaporation into hot air by turbulent mixed convection of heat and mass transfer in an insulated vertical channel. Hot air is flowing downward with concurrent flow of thin liquid water film falling on both sides of the channel walls as shown in Fig. 1. The channel walls are insulated in order to investigate the evaporative cooling, associated with the latent heat transport of film evaporation. The width of the channel is $2b$ and the thin liquid film flow is laminar and fed with an inlet temperature of T_{li} and a mass flow rate of B. The hot air stream is turbulent and enters the vertical channel with a fully developed velocity u_{f} obtained from a fully developed turbulent channel flow and a uniform temperature T_{o} assuming no water vapor within. The inlet temperature of the liquid film is always less than that of hot air stream. Apparently, the liquid film serves as a thermal protection from the hot air. The liquid film evaporates into the hot air stream as a result of the heat from the hot air transferring to the liquid film. Therefore, the thermal and solutal buoyancy forces are generated through the heat and mass transfer between hot air and liquid film, which is determined by the coupled transport process of the liquid and air. The turbulent air flow can be modified by these buoyancy forces with the shearing effect created by the falling film. In this study, a detailed numerical analysis is performed by simultaneously solving the conservation equations for various transport processes in the liquid film and turbulent hot gas flow with the interfacial matching conditions treated. An attempt has been made to model the process with the following simplifying assumptions:

1. Two-dimensional and boundary layer flow is considered for the hot gas flow.
2. The secondary effects such as radiation heat transfer, viscous dissipation effects are negligible.
3. The liquid film flow is laminar with a low mass flow rate such that the time-wise steady film thickness from former investigation [30,31] can be used. This steady film thickness can be interpreted as the temporal average of the large amplitude waves on the surface of the actual film [30].
4. The inertia terms in the momentum equation of the liquid film are small compared with the viscous term following Baumann and Thiele [15].
5. The gas–liquid interface is in thermodynamic equilibrium and semi-permeable [32]. That is, the solubility of air in the liquid film is negligibly small and the y-component of air velocity is zero at the interface.
6. The air–vapor mixture is an ideal gas mixture.

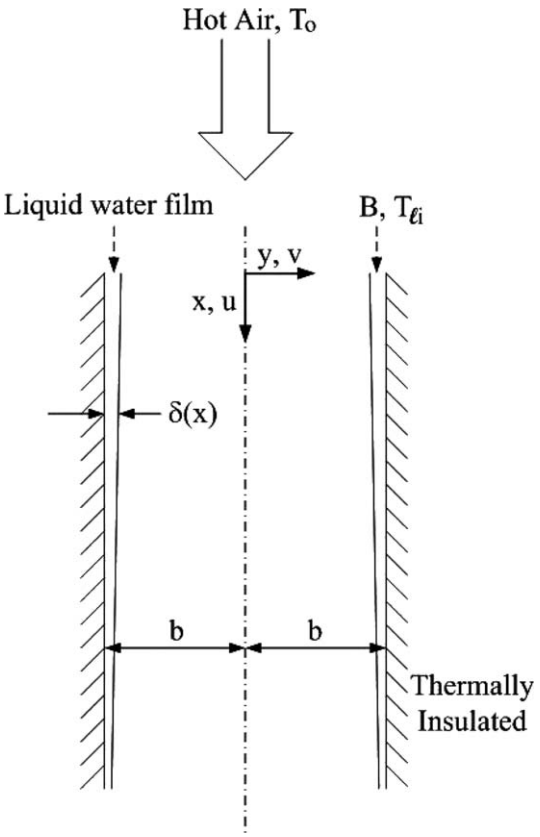

Fig. 1. Schematic diagram of the physical system.

2.1. Governing equations

2.1.1. Basic equations for the liquid film

With the assumptions mentioned above, the two-dimensional boundary layer flow steady laminar momentum and heat transfer equations for the liquid film can be expressed in the following equations:

Axial momentum equation

$$0 = \frac{\partial}{\partial y}\left(\mu_{\mathrm{l}}\frac{\partial u_{\mathrm{l}}}{\partial y}\right) + \rho_{\mathrm{l}} g \tag{1}$$

Energy equation

$$\rho_{\mathrm{l}} C_{p_{\mathrm{l}}} u_{\mathrm{l}} \frac{\partial T_{\mathrm{l}}}{\partial x} = \frac{\partial}{\partial y}\left(\lambda_{\mathrm{l}}\frac{\partial T_{\mathrm{l}}}{\partial y}\right) \tag{2}$$

2.1.2. Basic equations for the gas stream

Turbulent steady convection of heat and mass transfer in the gas flow can be explored by the following equations with the usual boundary layer approximations:

Continuity equation

$$\frac{\partial \rho u}{\partial x} + \frac{\partial \rho v}{\partial y} = 0 \tag{3}$$

Axial-momentum equation

$$\rho\left(u\frac{\partial u}{\partial x} + v\frac{\partial u}{\partial y}\right) = -\frac{\partial p_{\mathrm{m}}}{\partial x} + \frac{\partial}{\partial y}\left[(\mu + \mu_{\mathrm{t}})\frac{\partial u}{\partial y}\right] - (\rho_{\mathrm{o}} - \rho)g \tag{4}$$

Energy equation

$$\rho C_p\left(u\frac{\partial T}{\partial x}+v\frac{\partial T}{\partial y}\right)=\frac{\partial}{\partial y}\left[(\lambda+\lambda_t)\frac{\partial T}{\partial y}\right] \tag{5}$$

Concentration equation of water vapor

$$\rho\left(u\frac{\partial w}{\partial x}+v\frac{\partial w}{\partial y}\right)=\frac{\partial}{\partial y}\left[\rho(D+D_t)\frac{\partial w}{\partial y}\right] \tag{6}$$

where μ_t, λ_t, and D_t are the turbulent viscosity, conductivity and mass diffusivity of the binary gas mixture, respectively. It is noted in Eq. (4) that the third term on the right hand side represents the buoyancy forces due to the variations in temperature and concentration.

In the study of steady channel flow, an additional equation is necessary to solve the pressure gradient term in the axial momentum equation. The overall mass balance equation at each axial location is utilized to serve this purpose and expressed as the following:

$$\int_0^{b-\delta}\rho_g u_g\,dy=\rho_o\bar{u}_f(b-\delta_o)-\int_0^x\rho_g v_I\,dx \tag{7}$$

2.2. Boundary and interfacial conditions

The boundary conditions subject for equations of liquid film and gas stream, Eqs. (1)–(6), are as the following: at the channel wall the no-slip conditions for u and v have to be satisfied as well as the insulated wall condition. Due to the symmetry argument, all gradient in the mixture flow on the channel axis will be zero. The inlet conditions are fully developed velocity and flat temperature distribution with no water vapor.

The matching conditions at the gas–liquid interface, $y=b-\delta(x)$, are given as the following:

(1) continuities of velocity and temperature

$$u_I(x)=u_{g,I}=u_{l,I};\ T_I(x)=T_{g,I}=T_{l,I} \tag{8}$$

(2) continuities of shear stress

$$\tau_I(x)=\left[(\mu+\mu_t)\left(\frac{\partial u}{\partial y}\right)\right]_{g,I}=\left(\mu\frac{\partial u}{\partial y}\right)_{l,I} \tag{9}$$

(3) transverse velocity of the air–vapor mixture

$$v_I=-\frac{D+D_t}{1-w_I}\cdot\left(\frac{\partial w}{\partial y}\right)_I \tag{10}$$

(4) the mass fraction of the vapor

$$w_I=\frac{M_v p_I}{M_a(p-p_I)+M_v p_I} \tag{11}$$

where p_I is the partial pressure of the vapor at the gas–liquid interface. M_v and M_a are the molar mass of the water and air vapor, respectively.

(5) vaporizing flux of water vapor into the gas flow

$$\dot{m}''_I=-\rho v_I=\rho\frac{D+D_t}{1-w_I}\cdot\frac{\partial w}{\partial y} \tag{12}$$

(6) energy balance at the gas–liquid interface

$$\left(\lambda\frac{\partial T}{\partial y}\right)_{l,I}=\left[(\lambda+\lambda_t)\frac{\partial T}{\partial y}\right]_{g,I}+\dot{m}''_I h_{fg} \tag{13}$$

It is described from Eq. (13) that the energy at the interface can be transported into the gas stream in two modes. One is the sensible heat transfer through the gas temperature gradient, q''_{sI}, and the other is through the latent heat transfer via the liquid film vaporization, q''_{lI}. Therefore, the total interfacial heat transfer from the liquid film to the gas stream, q''_I, can be expressed as

$$q''_I=q''_{sI}+q''_{lI}=\left[(\lambda+\lambda_t)\frac{\partial T}{\partial y}\right]_{g,I}+\dot{m}''_I h_{fg} \tag{14}$$

The local Nusselt number along the gas–liquid interface is defined as

$$Nu_x=\frac{h\cdot 4b}{\lambda_g}=q''_I\cdot\frac{4b}{\lambda_g(T_I-T_b)} \tag{15}$$

It can also be written as

$$Nu_x=Nu_s+Nu_l \tag{16}$$

where Nu_s and Nu_l are the local Nusselt numbers for sensible and latent heat transfer, respectively, and evaluated by

$$Nu_s=q''_{sI}\cdot\frac{4b}{\lambda_g(T_I-T_b)} \tag{17}$$

and

$$Nu_l=q''_{lI}\cdot\frac{4b}{\lambda_g(T_I-T_b)} \tag{18}$$

In a similar manner, the local Sherwood number at the interface is defined as

$$Sh=h_M\cdot\frac{4b}{D}=\dot{m}''_I\cdot\frac{(1-w_I)\cdot 4b}{\rho_g D(w_I-w_b)} \tag{19}$$

It should be noted that the thermophysical properties of the gas mixture and liquid film in the above formulation are considered as variables with temperature and mixture composition. They are calculated from the pure component data by means of mixing rules [33,34] applicable to any multi-component mixtures. The pure component data [35] are approximated by polynomials in terms of temperature.

In order to improve the understanding of heat and mass transfer process, a non-dimensional accumulated mass evaporation rate is introduced as Ref. [27]:

$$M_r=\int_0^x\frac{\dot{m}''_I}{B}\,dx \tag{20}$$

3. Turbulence modeling

The k–ε turbulence model is utilized to compute the turbulent viscosity μ_t. Therefore, the transport equations

for the turbulent kinetic energy and turbulent energy dissipation must be included for the analysis. For simulation of turbulence in the gas flow, a modified low Reynolds number k–ε model developed by Myong et al. [36] and Myong and Kasagi [37] is adopted to eliminate the usage of wall function in the computation and thus k and ε at the film surface are 0. Therefore, this model permits direct integration of the transport equations to the gas–liquid interface. The equations of the modified low Reynolds number k–ε model are:

Turbulent kinetic energy equation

$$\rho\left(u\frac{\partial k}{\partial x}+v\frac{\partial k}{\partial y}\right)=\frac{\partial}{\partial y}\left[(\mu+\mu_t)\frac{\partial k}{\partial y}\right]+\mu_t\left(\frac{\partial u}{\partial y}\right)^2-\rho\varepsilon \tag{21}$$

rate of dissipation of turbulent kinetic energy equation

$$\rho\left(u\frac{\partial \varepsilon}{\partial x}+v\frac{\partial \varepsilon}{\partial y}\right)=\frac{\partial}{\partial y}\left[\left(\mu+\frac{\mu_t}{\varepsilon}\right)\frac{\partial \varepsilon}{\partial y}\right]+C_1\frac{\varepsilon}{k}\mu_t\left(\frac{\partial u}{\partial y}\right)^2-\rho C_2 f_2\frac{\varepsilon^2}{k} \tag{22}$$

where

$$\mu_t=\frac{\rho C_\mu f_\mu k^2}{\varepsilon};\quad f_2=\left(1-\frac{2}{9}e^{-\left(\frac{R_t}{6}\right)^2}\right)\left(1-e^{\frac{-Y}{5}}\right)^2;$$
$$f_\mu=\left(1+\frac{3.45}{\sqrt{R_t}}\right)\left(1-e^{\frac{-Y}{70}}\right);\quad R_t=\frac{k^2}{\varepsilon};$$
$$Y=\frac{(b-y-\delta)u^*}{v};\quad u^*=\sqrt{\frac{\tau_w}{\rho}} \tag{23}$$

and the other empirical constants taken the following values [36,37]:

$$\sigma_k=1.4;\quad \sigma_\varepsilon=1.3;\quad C_1=1.4;\quad C_2=1.8;\quad C_\mu=0.09 \tag{24}$$

4. Numerical approach

In this work, an implicit finite-difference scheme was used to solve the coupled Eqs. (1)–(6) using a marching solution procedure. There are 101 non-uniform grid points in the axial direction. In the transverse direction (y), 101

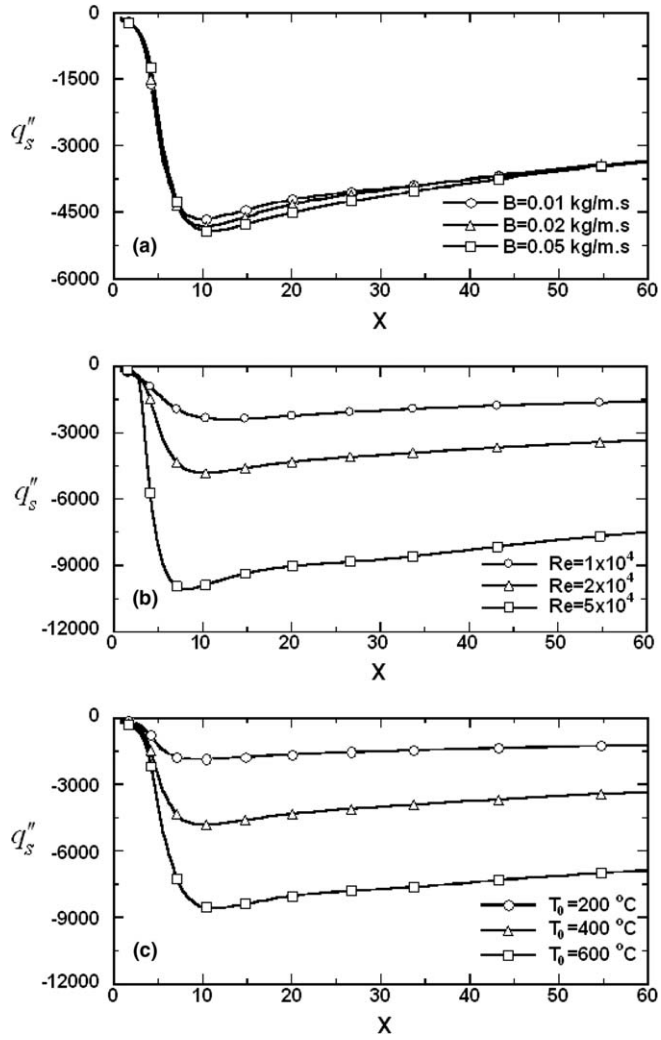

Fig. 2. Axial distribution of interfacial sensible heat flux with effect of (a) liquid flow rate, (b) Reynolds number, and (c) free stream temperature.

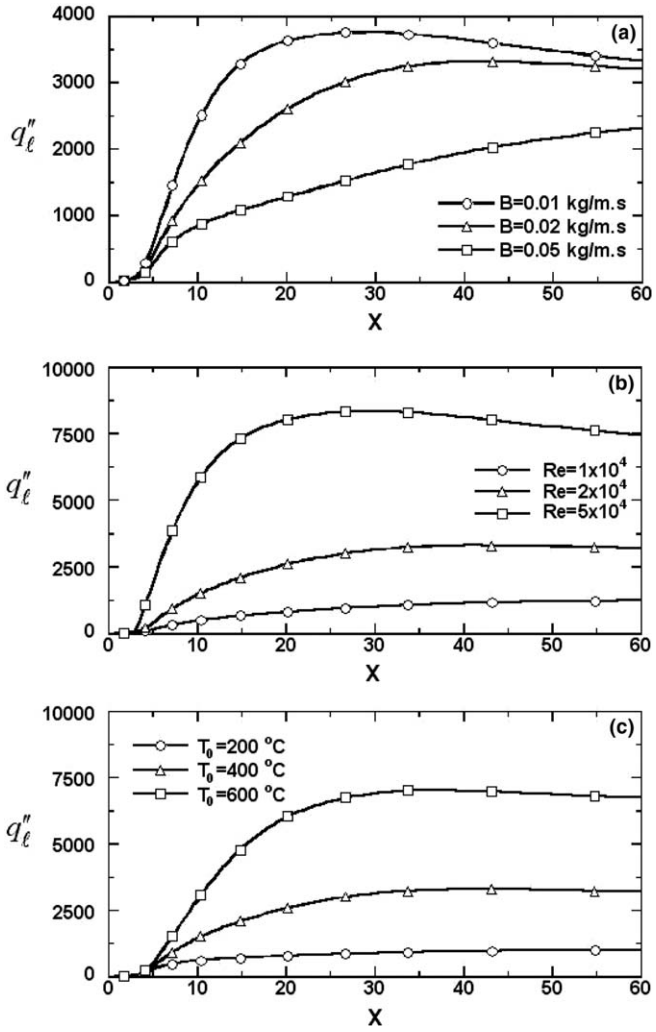

Fig. 3. Axial distribution of interfacial latent heat flux with effect of (a) liquid flow rate, (b) Reynolds number, and (c) free stream temperature.

non-uniform grid points were employed at the gas side and 21 non-uniform grid points were employed at the liquid side. The grids are transversely clustered near the gas–liquid interface, and the grid density is also higher in the region near the inlet. It was noted that the differences in the local Nusselt number, Nux, from computations using either $201 \times 201 \times 41$ or $101 \times 101 \times 21$ grids were always within 2%. Therefore, the $101 \times 101 \times 21$ grid was chosen for the subsequent computation. The governing equations are expressed in terms of finite difference approximations by employing the upstream difference in the axial convection terms and the central difference in the transverse convection and diffusion terms. The resulting system of algebraic equations can be cast into a tri-diagonal matrix equation, which can be solved by the TDMA method [38]. The matching condition imposed at the gas–liquid interface from Eqs. (8)–(13) are cast in backward difference for $(\partial\varphi/\partial y)_g$ and forward difference for $(\partial\varphi/\partial y)_l$ with φ denoting u to T. To check the adequacy of the numerical scheme used in this work, the results for the limiting case of turbulent mixed convection heat and mass transfer in a vertical wetted channel without consideration of the transport processes in the liquid film. Results were compared with those of Yan [39]. Excellent agreement between the present predictions and those of Yan [39] was found. The results for the limiting case of turbulent mixed convection heat transfer in a vertical pipe were also obtained. The predicted results agree with those of Tanaka et al. [40] and Cotton and Jackson [41]. In view of these validations, the present numerical algorithm and employed grid layout are adequate to obtain accurate results for practical purposes.

5. Results and discussion

Results of water film evaporation are presented in order to study the effects of flow conditions on the film cooling mechanism on the turbulent mixed convection heat and mass transfer in a vertical channel. A number of physical parameters such as the inlet film temperature, free stream

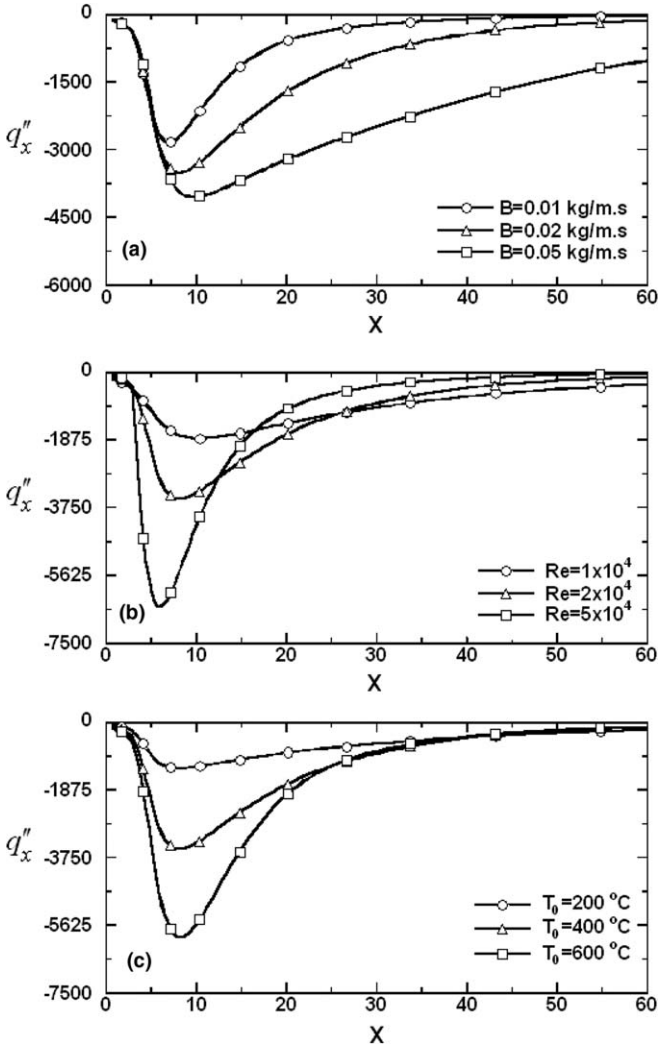

Fig. 4. Axial distribution of total interfacial heat flux with effect of (a) liquid flow rate, (b) Reynolds number, and (c) free stream temperature.

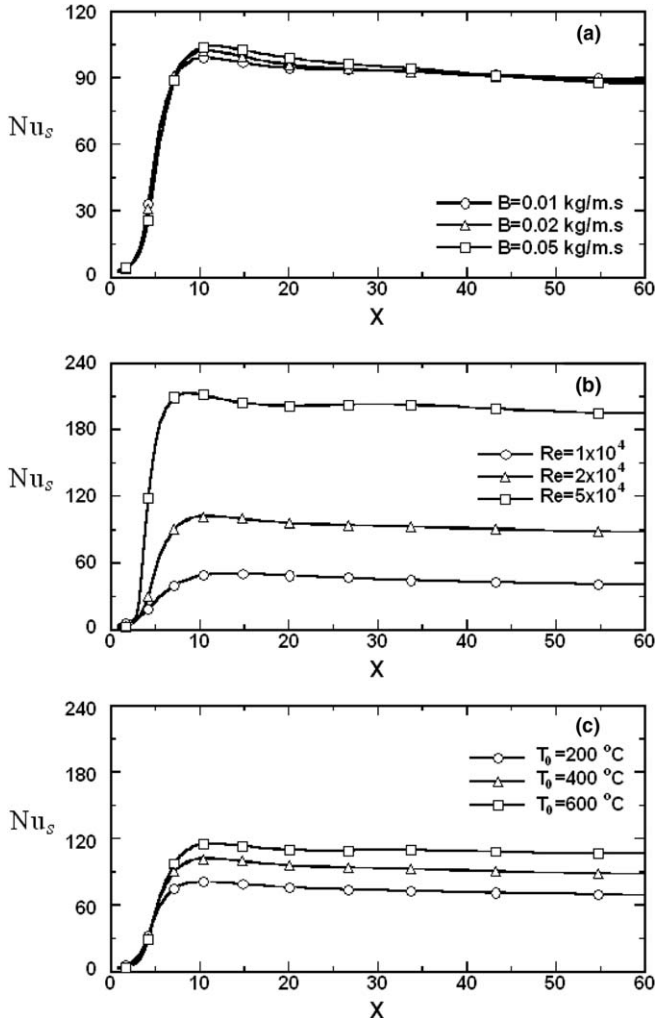

Fig. 5. Axial distribution of interfacial Nusselt number for sensible heat flux with effect of (a) liquid flow rate, (b) Reynolds number, and (c) free stream temperature.

temperature and velocity, liquid flow rate, channel width appear in this study. The parameters were varied systemically to examine the key trend in the results. The selected parameters are the liquid flow rate B, the free stream temperature T_o, and the Reynolds number Re due to their influences on the film cooling. The values of these parameters are 0.01, 0.02, and 0.05 kg/m s for B; 200, 400, and 600 °C for T_o and 1×10^4, 2×10^4, 5×10^4 for Re, respectively, where $B = 0.02$ kg/m s, $T_o = 400$ °C and $Re = 2\times10^4$ are selected for the base case. The inlet film temperature was remained fixed at 20 °C with the half-channel width of $b = 0.04$ m.

To study the relative contribution of the heat transfer through local sensible, latent and total heat flux, all the heat flux in the gas side with various effects are shown in Figs. 2–4, respectively. Fig. 2 presents the axial distributions of the interfacial sensible heat flux. The negative values of sensible heat flux represent that the direction of heat transfer is from the hot gas stream to the interface. It is seen that the sensible heat flux increases dramatically at the entrance ($X < 10$) and then decreases along the axial direction. An overall inspection of Fig. 2 reveals that the interfacial sensible heat flux increases as B, Re, and T_o increases, respectively. It also shows that the influences of Re and T_o on the sensible heat flux significantly. The axial distributions of the interfacial latent heat flux with various effects are shown in Fig. 3. Apparently, the values of the latent heat flux are all positive, and this indicates that the direction of the latent heat flux is from the interface to the hot gas stream. It is noted that the latent heat flux increases in the flow direction, with increasing Reynolds number and free stream temperature, but decreases as the liquid flow rate. This stems from the fact that larger convection is noted for a system with higher Reynolds number and temperature difference between liquid and gas. The reason for the decrease of latent heat flux with higher liquid flow rate is that the total internal energy stored in more liquid film resulted less evaporation. In Fig. 4, the total interfacial heat flux, the sum of interfacial sensible heat flux

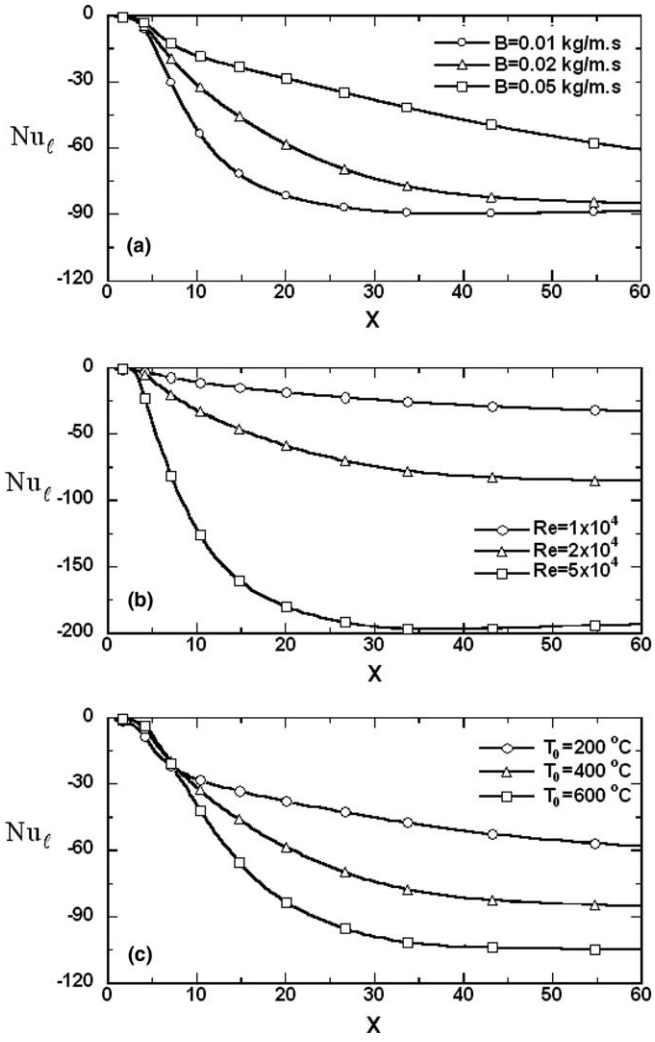

Fig. 6. Axial distribution of interfacial Nusselt number for latent heat flux with effect of (a) liquid flow rate, (b) Reynolds number, and (c) free stream temperature.

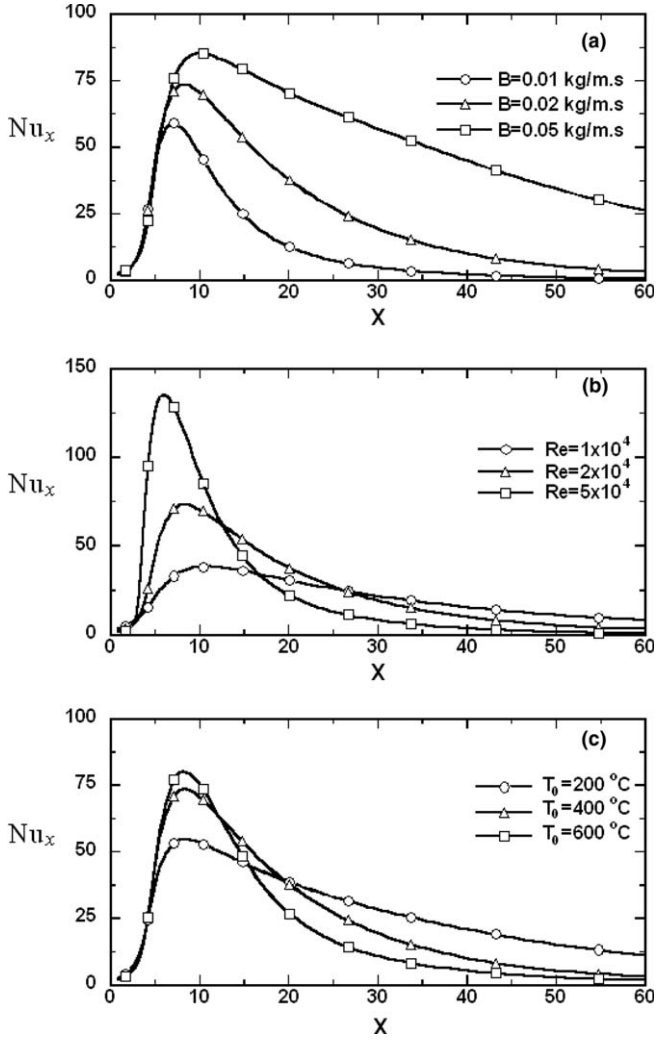

Fig. 7. Axial distribution of overall interfacial Nusselt number with effect of (a) liquid flow rate, (b) Reynolds number, and (c) free stream temperature.

and latent heat flux, is illustrated. It is observed that the effectiveness of protecting from the hot gas with liquid film is much better at the down stream.

For a better understanding of the interfacial heat transfer, the local Nusselt number for the sensible, latent and total heat flux with various effects are depicted in Figs. 5–7, respectively. In Fig. 5, Nu_s increases as B, Re, and T_o increases as sensible heat flux behaves. However, Nu_s remains almost constant at the downstream ($X > 20$). Fig. 6 presents the axial distribution of the local Nu_l. The negative values are resulted directed from its definition, Eq. (18). That is, a negative Nu_l implies that the direction of latent heat exchange is opposed to that of sensible heat exchange. It is found in Fig. 6 that the Nu_l increases with increasing Re and T_o, but with decreasing B. The same reason is explained as mentioned above. The Nu_x along the axial direction is shown in Fig. 7. This result clearly indicates that the magnitude Nu_s is much larger than that of Nu_l. It is interesting to see that the Nu_x increases as B, Re, and T_o increases near the entrance. However, the Nu_x increases with the decrease of Re and T_o at the downstream. This indicates that the liquid film helps lowering the heat transfer rate from the hot gas in the turbulent channel, especially at the downstream.

The distributions of the interfacial mass evaporation rate, Sherwood number and non-dimensional accumulation mass evaporation rate are presented in Figs. 8–10, respectively, for various effects to illustrate the mass transfer characteristics. It is apparent that the profiles are the same as that for latent heat flux. It is clear from Eq. (18) that the ratio of latent heat flux to the mass evaporation rate is the water latent heat. It is observed that a reduction of liquid flow rate causes greater film evaporation and there exists a maximum as the film evaporation is high. This is the result of decrease of the free stream temperature along the axial direction. The effects of B, Re, and T_o on the Sherwood number along the axial direction are illustrated in Fig. 9. It is clearly seen that the change in B has little effect on the Sherwood number and a larger Sherwood number is noted for systems with both higher Re and T_o. This is due to a smaller blowing effect for a smaller B and the larger interfacial evaporation rate for higher Re and T_o, which

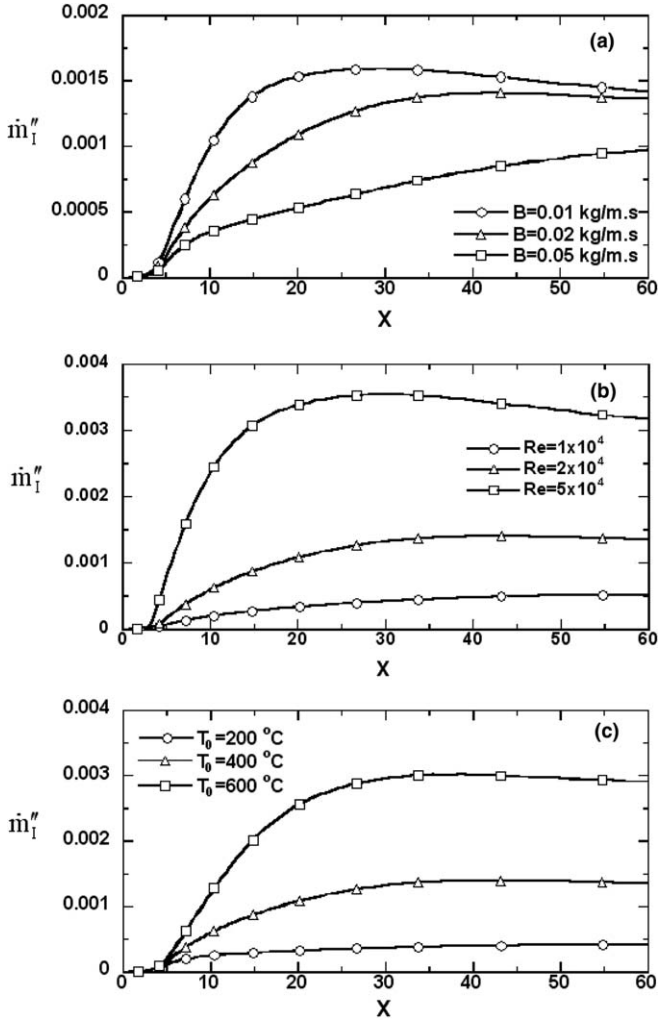

Fig. 8. Axial distribution of local evaporating mass flux with effect of (a) liquid flow rate, (b) Reynolds number, and (c) free stream temperature.

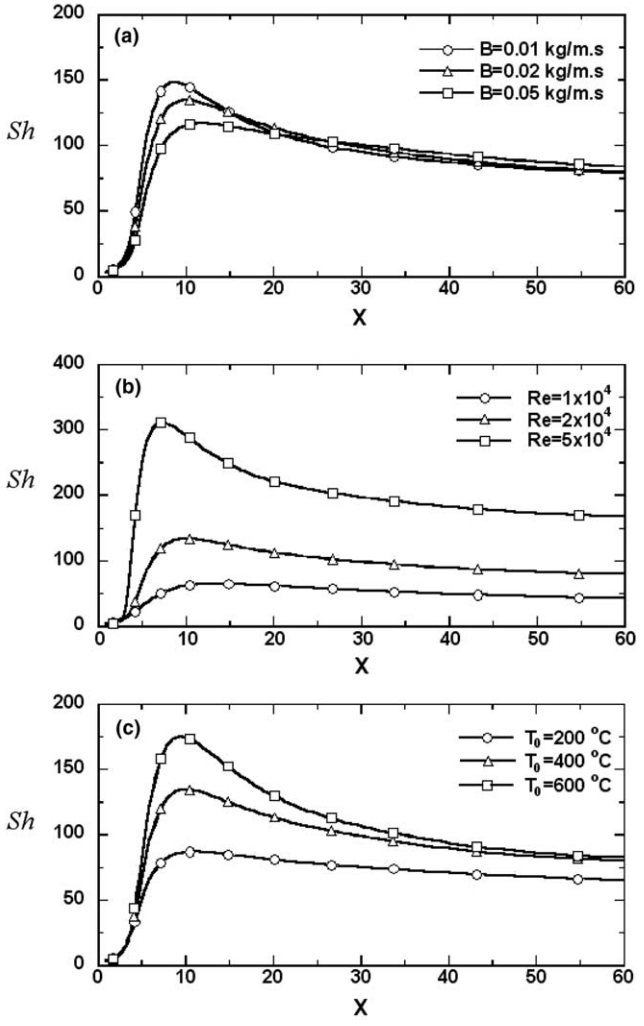

Fig. 9. Axial distribution of local Sherwood number with effect of (a) liquid flow rate, (b) Reynolds number, and (c) free stream temperature.

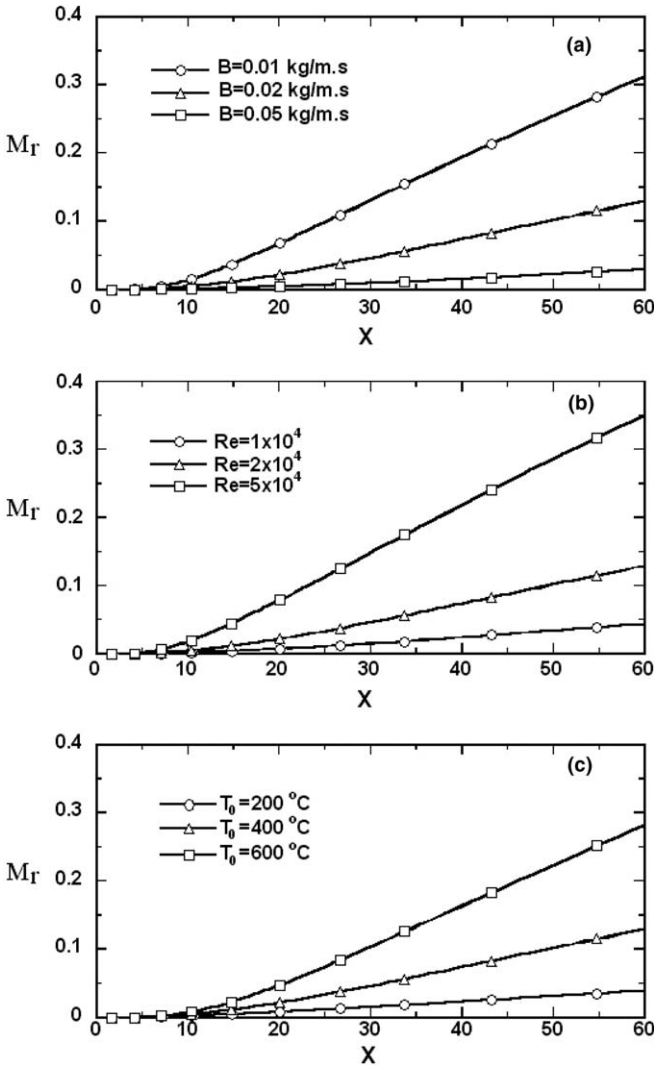

Fig. 10. Axial distribution of dimensionless accumulated evaporation rate with effect of (a) liquid flow rate, (b) Reynolds number, and (c) free stream temperature.

in turn results in a larger Sherwood number. The axial distributions of non-dimensional accumulated mass evaporation rate are shown in Fig. 10. It is clear that a reduction in B causes a larger M_r. The largest M_r is about 32%. It is also observed that M_r increases with increasing Re and T_o. The largest M_r with effects of Re and T_o are 35% and 28%, respectively.

6. Conclusions

The problem of a turbulent mixed convection of heat and mass transfer channel flow with film evaporation has been analyzed. The effects of liquid flow rate B, Reynolds number Re and free stream temperature T_o on heat and mass transfer have been studied in detail. Brief summaries of the major results are listed in the following:

1. As the liquid flow rate increases, the sensible heat flux increases, but the latent heat transfer decreases as well as the mass evaporation rate. This is due to a small blowing effect with higher liquid flow rate.
2. Higher Re and T_o cause a larger sensible and latent heat transfer as well as a better mass transfer.
3. The Nusselt number for total heat transfer increases as Re and T_o increases near the entrance, while decreases as Re and $T_o$increases at the down stream. This is because the direction of latent heat transfer is opposing to that of sensible heat transfer. This implies that the effectiveness of protection is better for higher Re and T_o.
4. The effect of B on the heat and mass transfer is insignificant, while the effects of Re and T_o are considerable.

Acknowledgements

The authors would like to acknowledge the financial support of the present work by the National Science Council, R.O.C. through the contract NSC 94-2212-E-211-004. The financial support from Northern Taiwan Institute of Science and Technology is also appreciated.

References

[1] G. Karimi, M. Kawaji, An experimental study of freely falling film in a vertical tube, Chem. Eng. Sci. 53 (1998) 3501–3512.
[2] W.W. Baumann, F. Thiele, Heat and mass transfer in two-component film evaporation in a vertical tube, The Eigth International Heat Transfer Conference, vol. 4, 1986, pp. 1843–1848.
[3] A. Ali Cherif, A. Daïf, Etude numérique du transfert de chaleur et de masse entre deux plaques planes verticals en présence dún film de liquide binaire ruisselant sur lúne des plaques chauffée, Int. J. Heat Mass Transfer 42 (1999) 2399–2418.
[4] S. Zheng, W.M. Worek, Method of heat and mass transfer enhancement in film evaporation, Int. J. Heat Mass Transfer 39 (1996) 97–108.
[5] W.M. Yan, T.F. Lin, Combined heat and mass transfer in natural convection between vertical parallel plates with film evaporation, Int. J. Heat Mass Transfer 33 (1990) 529–541.
[6] M. Asbik, O. Ansari, B. Zeghmati, Numerical study of boundary-layer transition in flowing film evaporation on horizontal elliptical cylinder, Numer. Heat Transfer A 48 (2005) 645–669.
[7] K.T. Lee, W.M. Yan, Mixed convection heat and mass transfer in radially rotating rectangular ducts, Numer. Heat Transfer A 34 (1998) 747–767.
[8] X.Q. Chen, J.C.F. Pereira, Prediction of evaporating spray in anisotropically turbulent gas flow, Numer. Heat Transfer A 27 (1995) 143–162.
[9] W.S. Fu, G.C. Yang, Influence of droplets' trajectories and size distribution on heat transfer from a wedge in an air–water mist flow, Numer. Heat Transfer A 16 (1989) 155–174.
[10] C.C. Huang, W.M. Yan, J.H. Jang, Laminar mixed convection heat and mass transfer in vertical rectangular ducts with film evaporation and condensation, Int. J. Heat Mass Transfer 48 (2005) 1772–1784.
[11] J.H. Jang, W.M. Yan, C.C. Huang, Mixed convection heat transfer enhancement through film evaporation in inclined square ducts, Int. J. Heat Mass Transfer 48 (2005) 2117–2125.
[12] C. Debbissi, J. Orfi, S. Ben Nasrallah, Evaporation of water by free convection in a vertical channel including effects of wall radiative properties, Int. J. Heat Mass Transfer 44 (2001) 811–826.
[13] E.H. Mezaache, M. Daguenet, Étude numérique de l'évaporation dans un courant d'air humide laminaire d'un film d'eau ruisselant sur une plaque inclinée, Int. J. Thermal Sci. 39 (2000) 117–129.

[14] T.R. Shembharkar, B.R. Pai, Prediction of film cooling with a liquid coolant, Int. J. Heat Mass Transfer 29 (1986) 899–908.
[15] W.W. Baumann, F. Thiele, Heat and mass transfer in evaporating two-component liquid film flow, Int. J. Heat Mass Transfer 33 (1990) 267–273.
[16] W.M. Yan, Evaporative cooling of liquid film in turbulent mixed convection channel flow, Int. J. Heat Mass Transfer 41 (1995) 3719–3729.
[17] Y.L. Tsay, T.F. Lin, Evaporation of a heated falling liquid film into a laminar gas stream, Exp. Therm. Fluid Sci. 11 (1995) 61–71.
[18] A.D. Carr, M.A. Connor, H.O. Buhr, Velocity, temperature, and turbulent measurement in air for pipe flow with combined free and forced convection, J. Heat Transfer 95 (1973) 445–452.
[19] M.A. Connor, A.D. Carr, Heat transfer in vertical tubes under conditioned of mixed free and forced convection, Sixth International Heat Transfer Conference, Toronto, Canada, vol. 2, 1978, pp. 43–48.
[20] B.P. Axcell, W.B. Hall, Mixed convection to air in a vertical pipe, Sixth International Heat Transfer Conference, Toronto, Canada, vol. 2, 1978, pp. 37–42.
[21] J.P. Easby, The effect of buoyancy on flow and heat transfer for a gas passing down a vertical pipe at low turbulent Reynolds numbers, Int. J. Heat Mass Transfer 21 (1978) 791–801.
[22] W.M. Yan, T.F. Lin, Y.L. Tsay, Evaporative cooling of liquid film through interfacial heat and mass transfer in a vertical channel—I. Experimental study, Int. J. Heat Mass Transfer 34 (1991) 1105–1111.
[23] W.M. Yan, T.F. Lin, Evaporative cooling of liquid film through interfacial heat and mass transfer in a vertical channel—II. Numerical study, Int. J. Heat Mass Transfer 34 (1991) 1113–1124.
[24] W.M. Yan, Effects of film evaporation on laminar mixed convection heat and mass transfer in a vertical channel, Int. J. Heat Mass Transfer 35 (1992) 3419–3429.
[25] W.M. Yan, Binary diffusion and heat transfer in mixed convection pipe flows with film evaporation, Int. J. Heat Mass Transfer 36 (1993) 2115–2123.
[26] M. Feddaoui, E. Belahmidi, A. Mir, A. Bendou, Numerical study of the evaporative cooling of liquid film in laminar mixed convection tube flows, Int. J. Therm. Sci. 40 (2001) 1011–1020.
[27] W.M. Yan, Effect of film vaporization on turbulent mixed convection heat and mass transfer in vertical channel, Int. J. Heat Mass Transfer 38 (1995) 713–722.
[28] S. He, P. An, J. Li, J.D. Jackson, Combined heat and mass transfer in uniformly heated vertical tube with water film cooling, Int. J. Heat Fluid Flow 19 (1998) 401–417.
[29] M. Feddaoui, A. Mir, E. Belahmidi, Concurrent turbulent mixed convection heat and mass transfer in falling film of water inside a vertical heated tube, Int. J. Heat Mass Transfer 46 (2003) 3497–3509.
[30] R.A. Seban, A. Faghri, Evaporation and heating with turbulent falling liquid films, J. Heat Transfer 98 (1976) 315–318.
[31] S.M. Yih, J.L. Liu, Prediction of heat transfer in turbulent falling films with or without interfacial shear, AIChE J. 29 (1983) 903–909.
[32] E.R.G. Eckert, R.M. Drake Jr., Analysis of Heat and Mass Transfer, McGraw-Hill, New York, 1972.
[33] R.B. Bird, W.E. Stewart, E.N. Lightfood, Transport Phenomena, Wiley, New York, 1960.
[34] R.C. Reid, J.M. Prausnitz, T.K. Sherwood, The Properties of Gas and Liquid, Hemisphere, McGraw-Hill, New York, 1977 (Chapter 11).
[35] T. Fujji, Y. Kato, K. Mihara, Expression of transport and thermodynamic properties of air, steam and water, Report No. 66, Department of Production Science, Kyushu University, Kyushu, Japan, 1977.
[36] H.K. Myong, N. Kasagi, M. Hira, Numerical prediction of turbulent pipe flow heat transfer for various Prandtl number fluids with the improved k–ε turbulence model, JSME Int. J. 32 (1989) 613–622.
[37] H.K. Myong, N. Kasagi, A new approach to the improvement of k–ε turbulence model for wall bounded shear flow, JSME Int. J. 33 (1990) 63–72.
[38] S.V. Patankar, Numerical Heat Transfer and Fluid Flow, Hemisphere, McGraw-Hill, New York, 1980.
[39] W.M. Yan, Turbulent mixed convection heat and mass transfer in a wetted channel, ASME J. Heat Transfer 117 (1995) 229–233.
[40] H. Tanaka, S. Maruyama, S. Hatano, Combined forced and natural convection heat transfer for upward flow in a uniformly heated vertical pipe, Int. J. Heat Mass Transfer 30 (1987) 165–174.
[41] M.A. Cotton, J.D. Jackson, Vertical tube air flows in the turbulent mixed convection regime calculated using a low-Reynolds number k–ε model, Int. J. Heat Mass Transfer 33 (1990) 275–286.